

Collapse of Neutrino Wave Functions under Penrose Gravitational Reduction

B.J.P. Jones¹ and O.H. Seidel¹

¹*University of Texas at Arlington, Arlington, Texas 76019, USA*

Models of spontaneous wave function collapse have been postulated to address the measurement problem in quantum mechanics. Their primary function is to convert coherent quantum superpositions into incoherent ones, with the result that macroscopic objects cannot be placed into widely separated superpositions for observably prolonged times. Many of these processes will also lead to loss of coherence in neutrino oscillations, producing observable signatures in the flavor profile of neutrinos at long travel distances. The majority of studies of neutrino oscillation coherence to date have focused on variants of the continuous state localization model, whereby an effective decoherence strength parameter is used to model the rate of coherence loss with an assumed energy dependence. Another class of collapse models that have been proposed posit connections to the configuration of gravitational field accompanying the mass distribution associated with each wave function that is in the superposition. A particularly interesting and prescriptive model is Penrose's description of gravitational collapse which proposes a decoherence time τ determined through $E_g\tau \sim \hbar$, where E_g is a calculable function of the Newtonian gravitational potential. Here we explore application of the Penrose collapse model to neutrino oscillations, reinterpreting previous experimental limits on neutrino decoherence in terms of this model. We identify effects associated with both spatial collapse and momentum diffusion, finding that the latter is ruled out in data from the IceCube South Pole Neutrino Observatory so long as the neutrino wave packet width at production is $\sigma_{\nu,x} \leq 2 \times 10^{-12}$ m.

I. INTRODUCTION

Neutrino oscillations [1] are a consequence of massive and mixed neutrinos acquiring different quantum phases as they travel over long baselines [2]. Neutrinos thus represent extremely sensitive quantum interferometers with which to study the structure of spacetime and the test the laws of quantum physics [3–6]. No violation of quantum mechanical unitary time evolution has yet been observed at the single particle level, in any system. Despite this, many have argued that they should be a strict necessity in order to resolve the measurement problem in quantum mechanics [7–9], ultimately providing a sound rational basis for explaining the emergence of definite outcomes when conscious observers interact with the Universe [10, 11]. Sensitive searches for this elusive “objective reduction” or collapse process using fundamental particles are thus highly motivated.

Neutrinos have been used to search for anomalous decoherence in a variety of experiments, and these analyses would in principle be sensitive to such violations [3, 12–17]. The results of these experiments are typically interpreted under continuous state reduction models [8, 18]. In this paper, we study the implications of these negative results for collapse theories based on gravitational mechanisms, specifically the model advanced by Penrose in Ref. [19]. While predicting broadly similar phenomena to continuous localization models, the mechanics outlined in Ref. [19] introduce additional subtleties into interpretation of the results in terms of the underlying model parameters. In particular, the collapse rate becomes dependent on the detailed geometry of the neutrino production process, which differs between experiments with different neutrino sources. At this time, we claim that enough is known about the expected wave packet sizes in neutrino oscillation experiments [20–25] that we can

confront the gravitational collapse model with data from contemporary neutrino oscillation experiments directly.

This paper is structured as follows. Section II schematically reviews the various possible sources of incoherence and decoherence in neutrino oscillations, briefly reviewing the Penrose prescription for gravitational collapse. Section III calculates the effects of the gravitational collapse model that are expected in neutrino oscillations. All of the relevant effects depend on the initial neutrino wave packet width, and we find upper bounds for the value that would be required for the effect to be observable in each type of experiment considered. Section IV compares the required wave packet sizes for each decoherence source against the theoretically expected values in a variety of neutrino experiments. Of those considered, only the IceCube South Pole Neutrino Observatory [3] has sensitivity to the Penrose model, via the effects of momentum de-localization associated with position-space collapse. The IceCube data does not support this model, as long as the wave packet size at production is smaller than $\sigma_{\nu,x} \leq 2 \times 10^{-12}$ m, which is consistent with expectations based on past calculations [21]. Finally, Section V summarizes our conclusions.

II. SOURCES OF INCOHERENCE AND DECOHERENCE IN NEUTRINO OSCILLATIONS

In this section, we outline the basic forms of neutrino coherence loss that may be expected in standard- and non-standard neutrino oscillations. Working in a two flavor model for illustration, a neutrino state $|\psi\rangle$ produced in flavor $|\nu_\alpha\rangle$ at time $t = t_0$ is comprised of a quantum superposition of mass state $|\nu_1\rangle$ and $|\nu_2\rangle$ with masses m_1

and m_2 with mixing matrix U , as

$$|\psi(0)\rangle = |\nu_\alpha\rangle \equiv \sum_i U_{\alpha i} |\nu_i\rangle. \quad (1)$$

The neutrino state vector evolves in time according to

$$|\psi(0)\rangle \rightarrow |\psi(t)\rangle = e^{-\frac{i}{\hbar} H t} |\psi(0)\rangle. \quad (2)$$

If we make the simplifying assumption that each ν_i is produced in an energy Eigenstate with energy E_i , then this becomes

$$|\psi(t)\rangle = \sum_i U_{\alpha i} e^{-\frac{i}{\hbar} E_i t} |\nu_i\rangle. \quad (3)$$

Evaluating the probability the neutrino will once again be found in state $|\nu_\alpha\rangle$ after time t amounts to projecting back onto the original flavor state to find the survival probability. For a simple two-flavor scenario we find the answer

$$P_{\alpha \rightarrow \alpha}(t) = |\langle \nu_\alpha | \psi(t) \rangle|^2 = 1 - \sin^2 2\theta \sin^2 \left(\frac{1}{2\hbar} [E_1 - E_2] t \right). \quad (4)$$

In the case where both mass states are in the same momentum basis state and the neutrino is fully relativistic such that $t = L$, we find $E_1 - E_2 \sim \Delta m^2 L / 2E$, resulting in the standard formula for neutrino oscillations,

$$P_{\alpha \rightarrow \alpha}(L) = 1 - \sin^2 2\theta \sin^2 \left(\frac{\Delta m^2 L}{4E} \right). \quad (5)$$

We have switched to natural units with $\hbar = c = 1$ and will use them for the rest of this paper. While we made an equal-momentum assumption for simplicity of notation, the same formula is also obtained if the neutrinos are not in equal momentum states but instead in the expected kinematic states produced from a common two- or three-body decay, as long as the wave packet separation effects discussed below are not significant.

An often un-stated assumption in this derivation is that it requires coherence to be maintained between the propagating mass states during their travel [26]. Loss of coherence amounts to an effective collapse of the wave function, for example,

$$|\psi(t)\rangle = \sum_i U_{\alpha i} e^{iE_i t} |\nu_i\rangle \rightarrow \begin{cases} e^{-iE_1 t} |\nu_1\rangle & P_1 = \cos^2 \theta \\ e^{-iE_2 t} |\nu_2\rangle & P_2 = \sin^2 \theta \end{cases} \quad (6)$$

where the two possible outcomes are realized with probability P_1 and P_2 , respectively. In this scenario the oscillatory behavior will be lost, and the flavor composition becoming invariant with distance, fixed at

$$P_{\alpha \rightarrow \alpha}(L) = \sum_i P_i |\langle \nu_\alpha | \nu_i \rangle|^2 = 1 - \frac{1}{2} \sin^2 2\theta. \quad (7)$$

There are multiple mechanisms by which loss of coherence can take place. One possibility is environmental

decoherence, whereby the neutrino becomes somehow entangled with an external system $|\epsilon\rangle$, such that

$$|\psi\rangle \rightarrow \sum_i U_{\alpha i} |\nu_i\rangle \otimes |\epsilon_i\rangle, \quad |\epsilon_i\rangle \neq |\epsilon_j\rangle. \quad (8)$$

Then the final state accompanying $|\nu_1\rangle$ is distinct from the final state accompanying $|\nu_2\rangle$, and the oscillation probability becomes

$$P_{\alpha \rightarrow \alpha}(L) = 1 - \sin^2 2\theta \left[\frac{1}{2} + \frac{1}{2} \mathcal{R} \langle \epsilon_1 | \epsilon_2 \rangle \cos \left(\frac{\Delta m^2 L}{2E} \right) \right]. \quad (9)$$

In the case where the environment entangled with $|\nu_1\rangle$ is very different to that entangled with $|\nu_2\rangle$, then $\langle \epsilon_1 | \epsilon_2 \rangle = 0$ destroying all interference. Equation 9 makes it clear that partial environmental decoherence is also possible for intermediate values of $\mathcal{R} \langle \epsilon_1 | \epsilon_2 \rangle$, which is relevant for scenarios where the environment gradually gains information about the mass states rather than resolving them in a single entangling interaction. Because neutrinos barely interact with their environments, environmental decoherence is not expected in any currently accessible experimental configuration. It may become relevant in exotic scenarios where entanglements develop with new beyond-standard-model background fields [27].

A second source of decoherence is wave packet separation. Neutrinos are not born in perfect momentum Eigenstates, but instead are produced as wave packets [26, 28], such that

$$|\psi\rangle = \sum_i U_{\alpha i} \int d^3 p \psi_i(p) |\nu_i, p\rangle, \quad (10)$$

where $|\nu_i, p\rangle$ is a mass eigenstate of mass m_i and momentum p and $\psi_i(p)$ is the wave function this mass state. In the proceeding sections we will follow the standard practice of assuming the wave functions can be well approximated by Gaussian functions, such that

$$\psi_i(p) = \frac{1}{\sqrt{2\pi\sigma^2}} \exp \left[-\frac{(p - p_0^i)^2}{4\sigma_{\nu,p}^2} \right]. \quad (11)$$

In this case the position-space wave function width can be related to the momentum-space one by the lower bound of the Heisenberg uncertainty principle,

$$\sigma_{\nu,x} \sigma_{\nu,p} = \hbar/2. \quad (12)$$

We note that caution must be exercised in applying relation 12 to neutrino wave packets, since $\sigma_{\nu,x}$ is the coherent spatial wave function width, often significantly smaller than the experimenter's uncertainty about the emission position of the neutrino. This distinction is discussed in some detail in Ref. [20].

Because the neutrino mass states are produced in a common decay process and the kinematics in the final state are distinct in each case, the central momenta p_0^i accompanying each mass state are nonequivalent. As the

wave packets propagate, they therefore travel with different group velocities. This means that eventually the wave functions accompanying each mass state will separate, and as they do so, oscillation coherence is lost. This phenomenon has been discussed at length in many past works, including but not limited to Refs. [20, 21, 26, 28–30]. The distance L_{coh} over which coherence becomes lost is related to the initial neutrino wave packet width $\sigma_{\nu,x}$ via

$$L_{coh} = 2\sqrt{2} \frac{\sigma_{\nu,x}}{\Delta v_{ij}}, \quad (13)$$

where Δv_{ij} is the velocity difference between neutrino mass eigenstates, $\Delta v = \Delta m^2/2E^2$. The major challenge with understanding the expected observable consequences of this coherence loss is the prediction of the initial state wave function width $\sigma_{\nu,x}$. This is a quantity that depends on the kinematics of the decay and the localization of the initial state by interactions with its environment, and has been calculated for several systems of interest including meson decay in accelerator neutrino beams [21], beta decay in nuclear reactors [21] and electron capture sources [22]. Although it also depends on the quantity $\sigma_{\nu,x}$, we stress that this standard “wave packet separation” effect is a distinct coherence loss mechanism to the one that is our main focus in this paper.

The decoherence phenomena described thus far occur for neutrinos obeying ordinary quantum mechanical time evolution. Additional losses of coherence may then be present, if there are fundamental violations of the unitary time evolution of quantum mechanics.

The non-standard collapse theories fall into two broad classes: spontaneous collapse models such as Ref. [7] which posit that there is a fundamental law acting to reduce superpositions into incoherent states directly; and collapse theories that postulate that the geometry of the gravitational field plays some specific role in the process. The first class of models is well represented by the continuous state localization model [8], under which superpositions are reduced to incoherent sums of their basis states in some basis at a specified rate. Its impact on neutrino oscillations has been explored in many works, such as Ref. [6, 15, 31–33]. The effect is a steady loss of coherence that suppresses off-diagonal elements in the flavor-space density matrix. Since the precise dynamics of state-localization are unknown, the effects of spontaneous collapse processes are typically modeled by introducing a set of operators with power-law energy dependence into the Lindblad equation for neutrino oscillations. A typical approach is to set limits on the possible magnitude of the decoherence strength Γ that multiplies each relevant Lindblad operator, scaling as

$$\Gamma = \Gamma_0 \times \left(\frac{E}{E_0} \right)^n, \quad (14)$$

with n as an unknown energy exponent [6] and E_0 a pivot energy that is chosen for convenience. The effective

dynamics of these models are often considered as representative of a broad class of models that include virtual black hole formation in spacetime foam [6, 34], deformation of symmetries [35, 36], metric perturbations [36, 37], fluctuating minimal lengths [36, 38] and light cone fluctuations [39]

Prototypical examples of models invoking the geometry of gravitational field to explain collapse include the Penrose model [19], the Diosi model [40, 41], and the Karolyhazy [42] model. In these approaches, the distinct spacetime metric curvatures that accompany different wave function components in superposition lead to a collapse. Penrose reasons in Ref. [19] that the characteristic energy scale for collapse would be given by

$$\begin{aligned} E_g &= \frac{1}{G} \int d^3x (\nabla\psi_2 - \nabla\psi_1)^2, & (15) \\ &= 4\pi \int d^3r (\psi_1 - \psi_2)(\rho_1 - \rho_2), & (16) \end{aligned}$$

where ψ_i is the gravitational potential associated with each mass distribution ρ_i in the superposition and G is Newtons constant. The decoherence time for these two distributions is found to be

$$\tau \sim 1/E_g. \quad (17)$$

This is motivated on the basis that states on spacetimes with different metrics will evolve into incompatible Hilbert spaces [19, 43], and as such, coherently interfering quantum states cannot be supported. Therefore, superpositions of states corresponding to significantly different gravitational curvatures must become collapsed, preventing large objects from existing in prolonged states of macroscopically separated superposition.

Applying this model to real materials used in experiments immediately runs into a challenging problem: for mass distributions that are truly point-like, expression 15 diverges. Penrose [43] and Diosi [40] propose distinct solutions to this problem. Penrose suggests that no particle in the real world has a truly point-like wave function, since evolution of its wave packet will disperse it until the point that gravity limits this spreading. Thus the prescribed approach is to apply the Schrödinger Newton equation [44], a nonlinear form of the Schrödinger equation that incorporates a gravitational self-attraction term between different parts of the wave function. This protocol delivers the equilibrated wave function width for the particle before collapse, after which Eq. 15 can be applied to the suitably broadened state. Diosi opts for a different solution, postulating a new fundamental length scale on which the mass distributions must be smeared in order to apply Eq. 15. The distance scale advocated by Diosi is in principle, an experimentally discoverable and fundamental quantity.

The avoidance of divergences originating from a point-like wave function, however, is not a relevant concern for any system where particles are produced with a non-trivial quantum mechanical width. This is the case in neutrino oscillation experiments. Ref. [18] suggests that the Penrose model cannot reasonably be applied to

neutrino oscillation system because the solution of the Schrödinger-Newton equation [44] leads to meaninglessly short decoherence distances in the case where the neutrino is allowed to reach this fully collapsed width. However, this misses a crucial point, that even if the neutrino wave packet width would ultimately become limited to the scale set by the Schrödinger Newton equation, it does not have time to spread to reach this width in experimental conditions. Instead, in all terrestrial experiments the neutrino wave packet width remains very close to its initial value during the neutrino flight time, since the dispersion effect is very slow, scaling as $(\Delta m^2)^2/E^4$. As such, for neutrino oscillations we can apply gravitational collapse models without applying an additional smearing effect, since the neutrino source determines the relevant coherent wave packet width. This is distinct from the assumptions made to treat macroscopic objects in Ref. [43], where it is assumed as a starting point that the equilibrium gravitationally collapsed width has been reached.

Neutrino widths emerging from the production process have now been calculated for many of the scenarios of experimental interest [20–22]. These predictions should provide sufficient information to apply the Penrose collapse model to predict neutrino coherence loss distances. Unlike in the continuous state reduction models, the gravitational collapse model couples the geometrical shape of the neutrino wave packet to its gravitational collapse, so the effects of standard wave packet separation and gravitational collapse must be considered together. Both of these effects acting as a function of $\sigma_{\nu,x}$ with distinct neutrino energy and baseline scalings. In the next section we calculate these effects.

III. EFFECTS OF GRAVITATIONAL COLLAPSE IN NEUTRINO OSCILLATIONS

The precise details of the collapse dynamics are not specified by Penrose’s approach. Nevertheless, the arguments leading to it can be extended to the neutrino oscillation system with some small and defensible extrapolations. We first note that for relativistic particles, gravitational curvature is sourced primarily by the energy rather than mass, so we consider the densities and potentials in Eq. 16 to be sourced by the energy-weighted distribution of $|\psi(x)|^2$ of the relativistic neutrino. This approach is consistent with the observation that in general relativity light rays gravitate towards each other with effective mass determined by the photon energy [45, 46], their energies serving as a source of metric curvature. A highly relativistic neutrino should behave rather similarly to a photon in terms of its gravitational dynamics. We also note that the Penrose prescription is not strictly Lorentz invariant since Eq. 17 involves the product of two timeline four-vector components. Since the mechanism purports to address the measurement problem in quantum mechanics, we perform the calculation in the observers rest frame, where whatever is considered to be

a “measurement” under this framework must presumably be executed. We now enumerate the effects that the gravitational collapse process is expected to have on coherence of oscillating neutrinos.

First, if we consider that the neutrino wave function is a sum of different neutrino mass states, each will lead to a distinct spacetime curvature due to the different magnitude of the mass in each case. This leads to a difference in self-energy that can be used to estimate a decoherence time. We call this **effect 1**, evaluated in Section III A. Second, neutrinos with different masses travel at different velocities and can separate spatially. This leads to a second contribution to the decoherence rate expected under the Penrose model which is more similar to the effects previously explored by Penrose *et.al.* for classical systems [19] and Bose Einstein Condensates [47]. We call this **effect 2**, evaluated in Sec III B. In practice, Effects 1 and 2 should be calculated simultaneously, and we present this combined calculation in Sec. III C. There is also a third, somewhat less direct source of coherence loss expected in this model. Since collapses in the position basis act to localize the spatial extent of the wave function, Heisenberg’s uncertainty principle demands they must also broaden it in momentum space. This leads to a stochastic contribution to the oscillation phase, which we term **effect 3**, evaluated in Sec. III D. In all of these cases, the magnitude of the effect depends on the spatial extent of the neutrino wave packet at production. Section IV evaluates the magnitude of the effect in various neutrino experiments based on the expected neutrino wave packet widths therein.

A. Effect 1: Collapse via neutrino mass difference

A given initial state produces neutrino mass basis states with slightly different energies and momenta to one another, with the energy and momentum differences calculable from kinematic considerations. The energy difference between two mass states produced is

$$\Delta E \sim \zeta \frac{\Delta m^2}{2E}, \quad (18)$$

where ζ is an order-1 number that is a function of the masses of the initial and final states [28]. To study **effect 1** in isolation from the other effects, we consider the case where the spatial difference between the two neutrino mass state wave packets is negligible, so $\psi_1 = \psi_2 = \psi$. Then we have

$$E_g = \frac{\Delta E_\nu^2}{G} \int d^3x (\nabla\psi)^2. \quad (19)$$

The gravitational potential for a mass density ρ is determined by Poisson’s equation,

$$\nabla^2\psi = 4\pi G\rho. \quad (20)$$

If we consider ρ to be a Gaussian distribution of width dictated by the width of the neutrino wave packet $\sigma_{\nu,x}$ [20] then it can be shown that the relevant potential is

$$\Phi = \frac{G}{4\pi} \frac{1}{r} \operatorname{erf} \left(\frac{r}{\sqrt{2}\sigma_{\nu,x}} \right), \quad (21)$$

which we can insert into Eq. 16,

$$E_g = \frac{\Delta E_\nu^2 G}{(2\pi)^{3/2} \sigma_{\nu,x}^3} \int d^3x \frac{1}{r} \operatorname{erf} \left(\frac{r}{\sqrt{2}\sigma_{\nu,x}} \right) \exp \left(\frac{r^2}{2\sigma_{\nu,x}^2} \right) \quad (22)$$

$$= \frac{\Delta E_\nu^2 G}{\sqrt{\pi} \sigma_{\nu,x}}. \quad (23)$$

Inserting Eq. 18, we find that the decoherence time is, in natural units,

$$\tau \sim 1/E_g = \frac{\sigma_{\nu,x}}{G} \left(\frac{2E_\nu}{\Delta m^2} \right)^2. \quad (24)$$

For highly relativistic neutrinos with $\tau \sim L$, this effect will become significant for wave packet sizes smaller than

$$\sigma_{\nu,x} \leq G \left(\frac{\Delta m^2}{2E_\nu} \right)^2 L. \quad (25)$$

This will be contrasted against expected wave packet sizes in contemporary experiments in Sec. IV.

B. Effect 2: Collapse via neutrino spatial separation

Not only are neutrino mass states produced with slightly different central energies, but they also travel with slightly different velocities [26]. This leads to a spatial separation that is a second source of wave function collapse. To estimate the magnitude of the effect, we can apply the estimate of E_g for hard sphere mass distributions calculated in Ref. [47],

$$E_g = \frac{GM^2}{R} \left(2\lambda^2 - \frac{3}{2}\lambda^3 + \frac{1}{5}\lambda^5 \right), \quad \lambda = \frac{b}{2R}. \quad (26)$$

where R is the sphere radius, which we take to be the wave packet width $\sigma_{\nu,x}$ and b is their separation, which will be given in terms of the velocity difference Δv_{ij} by

$$b = \Delta v_{ij} L = \frac{\Delta m^2}{2E^2} L. \quad (27)$$

Again we will take $M \sim E_\nu$, this time assuming a constant energy for both neutrino packets to investigate only the effect of their spatial separation and hence isolate **effect 2**. We thus arrive at

$$E_g = \frac{GE_\nu^2}{\sigma_{\nu,x}} \left(2\lambda^2 - \frac{3}{2}\lambda^3 + \frac{1}{5}\lambda^5 \right). \quad (28)$$

The decoherence time in the Penrose model for small separation $\lambda \ll 1$ is given by

$$\tau \sim 1/E_g = \frac{2\sigma_{\nu,x}^3}{GE_\nu^2 L^2} \left(\frac{2E_\nu^2}{\Delta m^2} \right)^2. \quad (29)$$

For a relativistic neutrino with $\tau \sim L$ we find the effect will be large for wave packet sizes that are small relative to their separation,

$$\sigma_{\nu,x} \leq \left[\frac{G}{8E_\nu^2} (\Delta m^2)^2 \right]^{1/3} L. \quad (30)$$

C. Combination of Effects 1 and 2

To rigorously account for effects 1 and 2, we need to incorporate them both simultaneously. A combined calculation using Gaussian wave packets yields

$$E_g = E_g^{(1)} + E_g^{(2)}, \quad (31)$$

$$E_g^{(1)} = \Delta E^2 \sqrt{\frac{2}{\pi}} \frac{G}{\sigma_{\nu,x}}, \quad (32)$$

$$E_g^{(2)} = 2E_\nu^2 G \left(\sqrt{\frac{2}{\pi\sigma^2}} - \frac{1}{b} \operatorname{erf} \frac{b}{\sqrt{2}\sigma^2} \right). \quad (33)$$

Since we are interested in small values of b we can Taylor expand $E_g^{(2)}$ to leading order, which gives

$$E_g^{(2)} \sim \frac{1}{3} \sqrt{\frac{2}{\pi}} \frac{E_\nu^2 G}{\sigma^3} b^2, \quad b = \left(\frac{\Delta m^2}{2E_\nu^2} \right) L. \quad (34)$$

We note that the effective collapse time from $E_g^{(1)}$ is identical to our earlier estimate of the contribution from **effect 1** derived in Sec III A, and the contribution from $E_g^{(2)}$ differs from the previous estimate for **effect 2** from Sec. IIIB only by a multiplicative numerical factor of $\frac{2\sqrt{2}}{3\sqrt{\pi}} = 0.53$, attributed primarily to the use of Gaussian rather than spherical wave packets. In all cases the magnitude of **effect 2** encoded in $E_g^{(2)}$ are far larger than magnitude of effect 1 that is encoded in $E_g^{(1)}$. As such, in subsequent sections we will find that the spatial decoherence that arises will always be dominated by effect 2, not by effect 1.

D. Effect 3: Decoherence via momentum delocalization

The phase of a neutrino that dictates oscillation is equal to the difference between the total accumulated phases of each mass state, which evolve as $e^{-iE_i t}$, where $E_i = \sqrt{p^2 + m_i^2}$. If the value of p were to change along the journey, the appropriate expression for the oscillation will instead become

$$\phi_{ij} = \int dt (E_i(t) - E_j(t)). \quad (35)$$

A steady localization in the position basis as generated by the gravitational collapse effect, whatever its microscopic origin, necessarily implies a steady delocalization in the momentum basis, as required by the Heisenberg principle. As such, if the collapse process is acting to localize the positions of the neutrino mass states it must be acting to delocalize their momenta. While the Penrose model does not provide the specific operators to use to implement this gravitational collapse, the conclusion is derived in a formal and general way in Ref. [48]: whenever a Lindblad operator depends on position, the expectation value of momentum is not constant. As such, the central momentum of the wave function will undergo random fluctuations, if collapses are allowed to occur. We note that such accelerations are also predicted to give rise to photon emission when applied to charged particles, and this effect has recently been searched for in low background underground experiments, in Refs [49, 50].

In the neutrino oscillation system, since two mass states are becoming distinguished by the collapse process, the random momentum perturbations will be independent for each mass basis state, since if they were not independent, the result would be the entire wave packet being translated in position space while maintaining its overall coherence. Thus we must consider that the central momentum of a given neutrino mass state at the time of measurement is inequivalent to its energy at the time of emission, such that

$$E_i = \sqrt{(p_0 + \delta p_i(t))^2 + m_i^2}. \quad (36)$$

Here we assume δp_i is a randomly fluctuating function, with a mean of zero $\langle \delta p_i \rangle = 0$. Assuming $\delta p_i, m_i \ll E_\nu$, we can expand,

$$E_i \sim E_\nu + \frac{2E_\nu \delta p_i + \delta p_i^2 + m_i^2}{2E_\nu}. \quad (37)$$

Where E_ν is the mean neutrino energy, averaged over mass basis states. To find the impact on the oscillation phase, we must evaluate the integral of Eq. 35,

$$\phi_{ij} = \frac{\Delta m^2}{2E_\nu} t + \int dt \left(\delta p_i(t) + \frac{\delta p_i^2(t)}{2E_\nu} \right). \quad (38)$$

The second term will tend to average to zero along the journey, because $\langle \delta p_i(t) \rangle = 0$. Oscillations will be decohered when the third term significantly de-phases the standard oscillation phase. This will be the case whenever

$$\delta \phi \equiv \frac{\int dt \langle \delta p_i^2(t) \rangle}{2E_\nu} \sim \mathcal{O}(1). \quad (39)$$

The RMS value of the momentum fluctuations $\Delta p = \sqrt{\langle \delta p_i^2 \rangle}$ is the momentum width that appears in the Heisenberg uncertainty principle due to the collapse process. To estimate this quantity, we note that the maximal coherent separation scale on which position superpositions may exist in this model is given by the b that

appears in Eq. 26. As such,

$$\Delta x \leq \sqrt{\frac{2\sigma_{\nu,x}^3}{GE_\nu^2 t}}. \quad (40)$$

This upper limit on coherent position uncertainty implies a lower limit to the momentum uncertainty, as

$$\Delta p \geq \frac{1}{2\Delta x} = \frac{1}{2} \sqrt{\frac{GE_\nu^2 t}{2\sigma_{\nu,x}^3}}, \quad (41)$$

The anomalous oscillation phase acquired from the dynamical position-space collapse is, from Eq. 39,

$$\phi \sim \frac{1}{16} \frac{GE_\nu L^2}{\sigma_{\nu,x}^3}, \quad (42)$$

which will be significant whenever

$$\sigma_{\nu,x} \leq \left(\frac{GE_\nu L^2}{16} \right)^{1/3}, \quad (43)$$

fixing the critical scale of $\sigma_{\nu,x}$ from **effect 3**.

IV. OBSERVABILITY OF GRAVITATIONAL COLLAPSE IN NEUTRINO EXPERIMENTS

All of the effects described above are observable only when the wave packet width at production $\sigma_{\nu,x}$ is suitably small. Each effect also has a distinct dependence on baseline and energy, motivating consideration of relative observability in various neutrino experiments. For the purpose of assessing observability, we consider the effect to be potentially detectable if it leads to a decoherence distance of at most $10\times$ the baseline of the experiment, thus yielding a 10% decohered neutrino flux. This appears to be a conservative criterion for detectability.

We compare the following cases, represented in terms of their approximate energy and baseline in Fig. 1:

- **Electron capture experiments:** The lowest energy experiments we consider are electron capture experiments. The BEST experiment [51] uses 50 tons of GaCl₃-HCl solution to radio-chemically detect electron neutrinos produced in electron capture decay of ⁵¹Cr. The experiment observed a deficit of neutrinos, confirming the previous anomalies of the SAGE and GALLEX experiments [52]. Explanations of the anomaly based on neutrino decoherence have been advanced in Refs. [53, 54]. The energies of the neutrinos in BEST emerge at four energies, energies; 747 keV (81.63%), 427 keV (8.95%), 752 keV (8.49%), and 432 keV (0.93%), shown as grey lines in Fig.1. For our estimations we use the flux-weighted mean of these values. The experiment is cylindrical, 2.34 m in height and 2.18 m in diameter, and we consider a representative neutrino baseline of 1 m. The expected wave

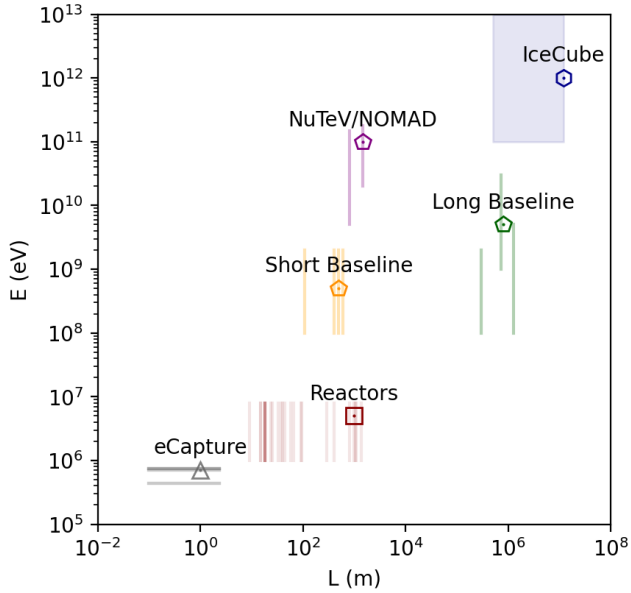


FIG. 1. Experiments considered in this section. The colored lines and boxes give a rough sketch of the energy and baseline spans of the relevant experiments, and the markers show the values we have taken as representative parameter points for each experiment class for subsequent calculations.

packet width in electron capture decays has been estimated for ${}^7\text{Be}$ to be 2.7 nm in Ref. [22], and a similar method can be used to predict the wave packet width in ${}^{51}\text{Cr}$ electron capture to yield a value of $\sigma_{\nu,x} \sim 70$ pm. The BeEST collaboration has recently published an experimental lower limit on the neutrino wave packet width in ${}^7\text{Be}$ decay of $\sigma_{\nu,x} \geq 2.7$ pm, still significantly smaller than the predicted value.

- **Nuclear reactors:** Nuclear reactors are copious neutrino sources. A wide variety of nuclear reactor neutrino experiments have operated at many different baselines [55]. An indication of non-standard reactor anti-neutrino disappearance was observed by comparing anti-neutrino fluxes from reactors to calculations, and finding the data to be anomalously low [56]. However, this anomaly has been confronted by new calculations of reactor fluxes that ameliorate the issue significantly [57]. As a representative reactor neutrino experiment we consider the operating parameters of the Daya Bay far detectors, which operate at 1 km baseline with a flux peaking at around 5 MeV [58]. The neutrino wave packet width expected in beta decay was studied in detail in Ref. [20]. The emitted neutrinos each have a different expected wave packet width that depends on the decaying isotope and the kinematics of the entangled final state particles, with $\sigma_{\nu,x} \sim 10 - 400$ pm widths expected. The Daya Bay collaboration has published an experimental

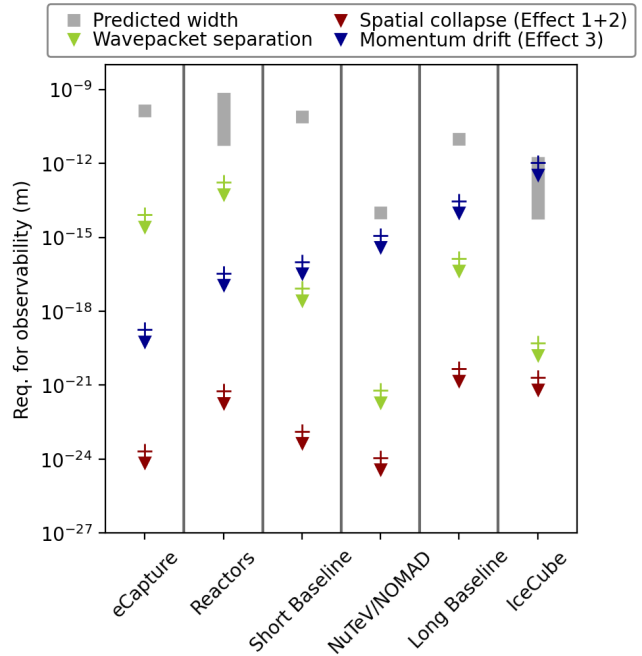


FIG. 2. Wave packet size required for observability of the effects in each experiment. The wave packet must be smaller than the indicated value for the effect to be observably large. The threshold for observability is conservatively considered to be the point when the decoherence distance is ten times the experiment baseline.

lower limit on the effective flux-averaged neutrino wave packet width [23], though it does not exclude the currently predicted value. Fig. 1 shows the red lines indicating the baselines of each of the reactor experiments described in [56] plus Daya Bay [59], RENO [60] and Double Chooz [61] experiments, alongside the approximate energy spread of the reactor anti-neutrino spectra.

- **Short Baseline Experiments:** Short baseline neutrino oscillation experiments such as MiniBooNE [62], MicroBooNE [63], SBND [64] and ICARUS [65] (shown as orange lines in Fig. 1) detect neutrinos produced in beams of magnetically focused hadrons created by proton collisions on solid targets. The charged hadrons travel through air as they decay, and interactions with the air molecules generate entanglements that quantum mechanically localize the neutrino parent. The emerging neutrino wave packet width has been calculated in Ref. [21]. For illustration of the scale of effect at these experiments we use the MiniBooNE experiment, which sits at a baseline of 500 m from the Fermilab Booster Neutrino Beam [66], with a flux-averaged detected neutrino energy of around 500 MeV [67]. The expected wave packet width for neutrinos of this energy in a conventional neutrino beam is approximately 8×10^{-11} m [21].

- **NuTeV/NoMAD:** Historically, much higher energy short baseline neutrino experiments have been operated using conventional neutrino beams. The NuTeV experiment [68] operated with a neutrino flux spanning a range of 20-180 GeV at a baseline of 1420 m at Fermilab. NOMAD operated with a similar beam energy range with an 825 m baseline at CERN. Both are shown as purple lines on Fig. 1. We take 100 GeV as a representative neutrino energy in these experiments for subsequent calculations. The beam production process resembles that of the short baseline experiments, albeit at much higher energies. The results of Ref. [21] imply a wave packet width for these experiments of approximately 8×10^{-14} m.
- **Long Baseline Experiments:** Accelerator neutrino experiments operating at longer baselines have a natural advantage when searching for weak, distance-dependent decoherence processes. Examples include MINOS [69], OPERA [70], NOvA [71], T2K [72] and DUNE [73], with baselines and approximate neutrino energy ranges shown as green lines on Fig. 1. The neutrino fluxes for these experiments are produced using the conventional hadron beam method, so the expected wave packet widths follow expectations from Ref. [21]. As a representative example we consider a 5 GeV beam propagating 735 km, reflecting the approximate operating parameters of the MINOS experiment. In these conditions the expected wave packet width is approximately 10^{-11} m.
- **IceCube:** The longest baseline and highest energy neutrino oscillation analyses currently available come from IceCube, which recently set strong limits on anomalous decoherence in Ref. [3]. The IceCube neutrino baselines depend on zenith angle and span a range of values from a few hundred km to the diameter of the Earth, 12,000 km. The energy spectrum of the sample studied in Ref. [3] peaks at 1 TeV, and the energy span of the IceCube samples is roughly indicated as a shaded blue box in Fig. 1. The neutrino wave packet width expected from production in atmospheric air showers has not yet been calculated explicitly. Since the particles are produced in pion and kaon decay, a rough scale can be inferred from the accelerator beamline calculations of [21], though with large error bars due to the rather different density of the atmosphere to that of the accelerator beam pipes. On the basis of those estimates we consider a viable range of plausible wave packet widths to be between 10^{-14} m $< \sigma_{\nu,x} < 10^{-12}$ m.

The maximal wave packet widths for observability of natural Penrose-model decoherence effects are shown in Fig. 2, compared against the calculated or estimated wave packet widths in the relevant experiments. No effect is expected from the mass curvature effect (**effect 1**),

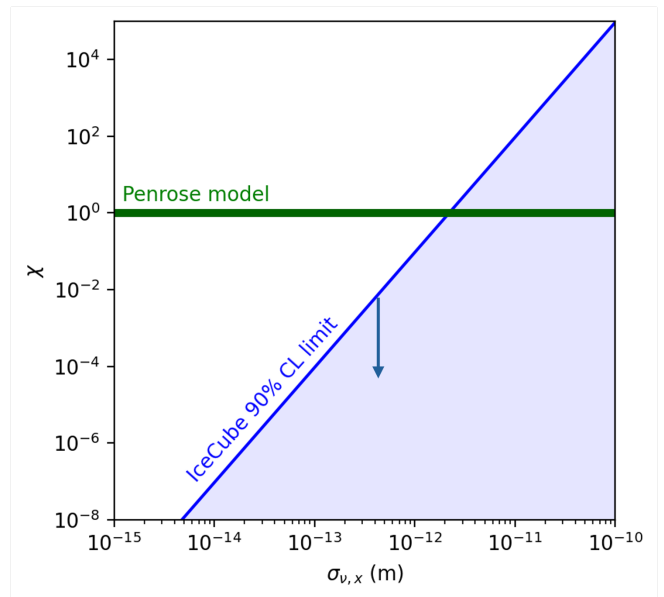


FIG. 3. Limit on the effective decoherence scaling parameter χ compared against the Penrose model expectation $\chi \sim 1$. The IceCube limit on Γ from Ref. [3] has been re-expressed as a constraint on χ and $\sigma_{\nu,x}$ by noting that this is a decoherence mechanism scaling as $\Gamma \propto E^{1/2}$, at which the coherence distance at 1 TeV has been constrained to be less than $L_{coh} \leq 30$ Earth diameters.

which is in all cases too low to show on the figure. Neither is any experiment sensitive to pure position-space collapse (**effect 2**). However, the momentum drift (**effect 3**) that is analogous to the expected heating effect in germanium experiments [49, 50] appears to within the IceCube sample sensitivity. We also show for comparison the wave packet width required for the standard wave packet separation effect encoded in Eq. 13. For the lower energy experiments such as electron capture and reactors, we find that wave packets will already be far separated by the time the Penrose-like collapse process could occur, so it is intrinsically unobservable in oscillations of these neutrinos. Due to the different energy and baseline scaling of the gravitational collapse vs wavepacket separation effects, for higher energy experiments the gravitational collapse becomes dominant over the standard wave packet separation effects.

To consider the quantitative extent to which this model is addressed by IceCube data, we note that the neutrino energy dependence of **effect 3** is that the coherence distance scales as

$$L \sim 4 \sqrt{\frac{\sigma_{\nu,x}^3}{GE}}, \quad (44)$$

which corresponds to a model with Γ scaling as $E_\nu^{1/2}$ in the notation of Ref. [3]. The 90% confidence level (CL) limit on the coherence length L_{90} under such a model can be evaluated based on the information provided in Ref. [3] to be approximately 30 Earth diameters at a

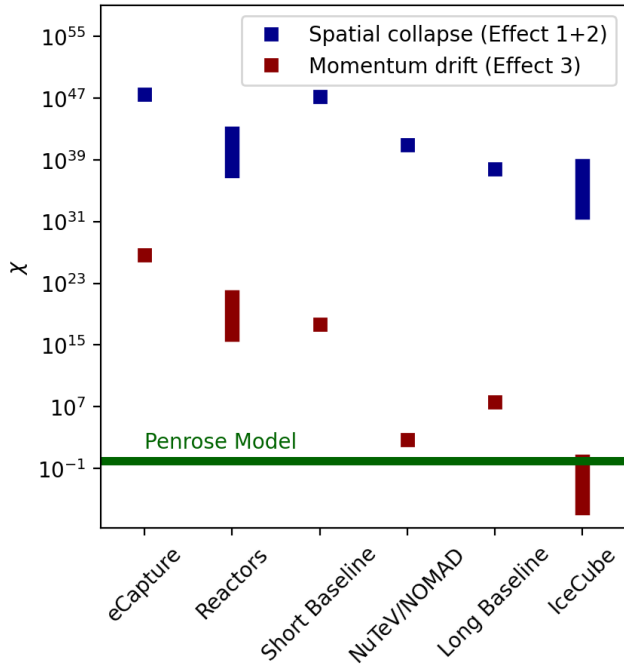


FIG. 4. Effective constraint on the Penrose model strength parameter χ for cases where the coherence length is constrained to be 10 times the size of the experimental baseline.

neutrino energy of $E_\nu \sim 1$ TeV. To quantify the strength of the limit on the Penrose model, a scaling parameter χ is inserted into Eq 17 to represent the strength of decoherence relative to the Penrose prescription, with $\chi \sim 1$ corresponding to the natural Penrose model and $\chi > 1$ representing stronger collapse effects, as

$$\tau \sim \frac{1}{\chi E_g}. \quad (45)$$

The limit obtained in Ref. [3] can then be re-expressed as an excluded region in the space of $\sigma_{\nu,x}$ and χ , via

$$\chi \leq \frac{16\sigma_{\nu,x}^3}{GE_\nu L_{90}^2}. \quad (46)$$

The allowed region is shown in Fig. 3. The neutrino wave packet would need to be larger than 2×10^{-12} m for the spontaneous collapse process to be unobservable in IceCube. To conclusively rule out this possibility, a full calculation of the expected neutrino wave packet width in atmospheric neutrino oscillation experiments would be required, though based on past calculations a value wider than 2×10^{-12} m seems unlikely. We defer a rigorous calculation of the wave packet width in atmospheric neutrino production processes to future work.

The expected effective strength χ that can be accessed in various experiments through both the spatial (**effect 2**) and momentum (**effect 3**) mechanisms are shown in Fig. 4, evaluated for hypothetical cases where

coherence length limits are conservatively set to 10 times the oscillation baseline. It is striking that the y axis on this plot spans more than sixty orders of magnitude. The momentum diffusion effect is much larger than the position collapse effect, since the former does not require the wave packets to separate substantially before it has an impact - the fact it restricts the spatial extent of the superposition necessary imposes momentum uncertainty, via the Heisenberg principle. Once again we observe that the higher energy experiments have a clear advantage, with IceCube spanning sensitivities beyond the Penrose natural model for the momentum-space effect. The NuTeV/NOMAD class of experiments come close this benchmark as well, approaching the sensitivity of the far longer baseline IceCube search due to their smaller expected wave packet widths. We note that a re-analysis of the data from those experiments in the context of the Penrose model could exceed the performance estimate presented here, due to the significant simplifying assumptions made in our estimates.

V. CONCLUSIONS

We have studied the expected effects of the Penrose gravitational collapse model on neutrino oscillations. While superficially similar to the continuous localization models commonly employed in neutrino decoherence analyses, the Penrose model introduces additional subtleties into the calculation by coupling the geometrical form and separation of the neutrino wave packet to its collapse rate.

We identify two main contributions to the expected decoherence rates under this model. The first is a purely spatial collapse which is similar to the mechanism originally proposed to forbid objects in macroscopic superpositions. This effect is dominated by the contribution from separation of the wave packets in space rather than the difference in their masses, but is very far from being observable given expected wave packet sizes in realistic neutrino emission processes. The second is a diffusive effect on the central neutrino momentum which leads to loss of oscillation phase coherence as the neutrinos are localized spatially. This effect is unobservable in the majority of experiments, but is addressed by IceCube decoherence analysis [3] at 90% CL as long as the wave packet size at production in air showers is less than $\sigma_{\nu,x} \leq 2 \times 10^{-12}$ m.

VI. ACKNOWLEDGEMENTS

We are grateful to Stuart Hameroff and co-organizers for hosting The 2024 Science of Consciousness conference, where this paper was conceived and written. We thank to Maria Startseva and Tyler Bryan for a series of beneficial Transmissions, and Tom Stuttard, Carlos Argüelles, Jonathan Asaadi and Varghese Chirayath for useful comments on this manuscript. BJJ is supported by the US

-
- [1] Masaharu Tanabashi, Particle Data Grp, K Hagiwara, K Hikasa, Katsumasa Nakamura, Y Sumino, F Takahashi, J Tanaka, K Agashe, Giulio Aielli, et al. Review of particle physics. *Physical Review D*, 98(3), 2018.
- [2] Carlo Giunti and Chung W Kim. *Fundamentals of neutrino physics and astrophysics*. Oxford university press, 2007.
- [3] Search for decoherence from quantum gravity with atmospheric neutrinos. *Nature Physics*, pages 1–8, 2024.
- [4] Neutrino interferometry for high-precision tests of lorentz symmetry with icecube. *Nature physics*, 14(9):961–966, 2018.
- [5] Roland M Crocker, Carlo Giunti, and Daniel J Mortlock. Neutrino interferometry in curved spacetime. *Physical Review D*, 69(6):063008, 2004.
- [6] Thomas Stuttard and Mikkel Jensen. Neutrino decoherence from quantum gravitational stochastic perturbations. *Physical Review D*, 102(11):115003, 2020.
- [7] Gian Carlo Ghirardi, Alberto Rimini, and Tullio Weber. Unified dynamics for microscopic and macroscopic systems. *Physical review D*, 34(2):470, 1986.
- [8] Angelo Bassi, Kinjalk Lochan, Seema Satin, Tejinder P Singh, and Hendrik Ulbricht. Models of wave-function collapse, underlying theories, and experimental tests. *Reviews of Modern Physics*, 85(2):471, 2013.
- [9] Steven Weinberg. *Lectures on quantum mechanics*. Cambridge University Press, 2015.
- [10] Stuart Hameroff and Roger Penrose. Consciousness in the universe: A review of the orch or theory. *Physics of life reviews*, 11(1):39–78, 2014.
- [11] Stuart R Hameroff and Roger Penrose. Consciousness in the universe an updated review of the “orch or” theory. *Biophysics of Consciousness: A Foundational Approach*, pages 517–599, 2017.
- [12] Stephen L Adler. Remarks on a proposed superkamiokande test for quantum gravity induced decoherence effects. *Physical Review D*, 62(11):117901, 2000.
- [13] Dan Hooper, Dean Morgan, and Elizabeth Winstanley. Probing quantum decoherence with high-energy neutrinos. *Physics Letters B*, 609(3-4):206–211, 2005.
- [14] A. L. G. Gomes, R. A. Gomes, and O. L. G. Peres. Quantum decoherence and relaxation in long-baseline neutrino data. *Journal of High Energy Physics*, 2023(10):35, 2023.
- [15] Valentina De Romeri, Carlo Giunti, Thomas Stuttard, and Christoph A Ternes. Neutrino oscillation bounds on quantum decoherence. *Journal of High Energy Physics*, 2023(9):1–24, 2023.
- [16] E Lisi, Antonio Marrone, and Daniele Montanino. Probing possible decoherence effects in atmospheric neutrino oscillations. *Physical Review Letters*, 85(6):1166, 2000.
- [17] JA Carpio, Eduardo Massoni, and AM Gago. Testing quantum decoherence at dune. *Physical Review D*, 100(1):015035, 2019.
- [18] Sandro Donadi, Angelo Bassi, Luca Ferialdi, and Catalina Curceanu. The effect of spontaneous collapses on neutrino oscillations. *Foundations of Physics*, 43:1066–1089, 2013.
- [19] Roger Penrose. On gravity’s role in quantum state reduction. *General relativity and gravitation*, 28:581–600, 1996.
- [20] BJP Jones, E Marzec, and J Spitz. Width of a beta-decay-induced antineutrino wave packet. *Physical Review D*, 107(1):013008, 2023.
- [21] Benjamin James Poyner Jones. Dynamical pion collapse and the coherence of conventional neutrino beams. *Physical Review D*, 91(5):053002, 2015.
- [22] Ben Jones. The width of an electron-capture neutrino wave packet (a.k.a. the number of the beast). 2024.
- [23] Daya Bay Collaboration. Study of the wave packet treatment of neutrino oscillation at daya bay. *The European Physical Journal C*, 77:1–14, 2017.
- [24] Joseph Smolsky, Kyle G Leach, Ryan Abells, Pedro Amaro, Adrien Andoche, Keith Borbridge, Connor Bray, Robin Cantor, David Diercks, Spencer Fretwell, et al. Direct experimental constraints on the spatial extent of a neutrino wavepacket. *arXiv preprint arXiv:2404.03102*, 2024.
- [25] Carlos A Argüelles, Toni Bertólez-Martínez, and Jordi Salvado. Impact of wave packet separation in low-energy sterile neutrino searches. *Physical Review D*, 107(3):036004, 2023.
- [26] E Kh Akhmedov and A Yu Smirnov. Paradoxes of neutrino oscillations. *Physics of Atomic Nuclei*, 72:1363–1381, 2009.
- [27] José F Nieves and Sarira Sahu. Neutrino decoherence in a fermion and scalar background. *Physical Review D*, 100(11):115049, 2019.
- [28] Carlo Giunti and Chung W Kim. Coherence of neutrino oscillations in the wave packet approach. *Physical Review D*, 58(1):017301, 1998.
- [29] Carlo Giunti. Neutrino wave packets in quantum field theory. *Journal of High Energy Physics*, 2002(11):017, 2002.
- [30] Mikael Beuthe. Towards a unique formula for neutrino oscillations in vacuum. *Physical Review D*, 66(1):013003, 2002.
- [31] JA Carpio, E Massoni, and AM Gago. Revisiting quantum decoherence in the matter neutrino oscillation framework. *Phys. Rev. D*, 97(11):115017, 2018.
- [32] AM Gago, Edivaldo Moura Santos, Walter Jose da Costa Teves, and R Zukanovich Funchal. A study on quantum decoherence phenomena with three generations of neutrinos. *arXiv preprint hep-ph/0208166*, 2002.
- [33] Gabriela Barenboim and Alberto M Gago. Quantum decoherence effects: a complete treatment. *arXiv preprint arXiv:2402.03438*, 2024.
- [34] SW Hawking. Spacetime foam. *Nuclear Physics B*, 144(2-3):349–362, 1978.
- [35] Michele Arzano, Vittorio D’Esposito, and Giulia Gubitosi. Fundamental decoherence from quantum spacetime. *Commun. Phys.*, 6(1):242, 2023.
- [36] Vittorio D’Esposito and Giulia Gubitosi. Constraints on quantum spacetime-induced decoherence from neutrino oscillations. 6 2023.

- [37] Ertan Goklu, Claus Lammerzahl, and Heinz-Peter Breuer. Metric fluctuations and decoherence. In *12th Marcel Grossmann Meeting on General Relativity*, pages 2420–2422, 7 2009.
- [38] Luciano Petruzzello and Fabrizio Illuminati. Quantum gravitational decoherence from fluctuating minimal length and deformation parameter at the Planck scale. *Nature Commun.*, 12(1):4449, 2021.
- [39] Thomas Stuttard. Neutrino signals of lightcone fluctuations resulting from fluctuating spacetime. *Physical Review D*, 104(5):056007, 2021.
- [40] Lajos Diosi. A universal master equation for the gravitational violation of quantum mechanics. *Physics Letters A*, 120(8):377–381, 1987.
- [41] Mohammad Bahrami, Andrea Smirne, and Angelo Bassi. Role of gravity in the collapse of a wave function: A probe into the diósi-penrose model. *Physical Review A*, 90(6):062105, 2014.
- [42] Roger Penrose and Chris J Isham. Quantum concepts in space and time. 1986.
- [43] Roger Penrose. On the gravitization of quantum mechanics I: Quantum state reduction. *Foundations of Physics*, 44:557–575, 2014.
- [44] Mohammad Bahrami, André Großardt, Sandro Donadi, and Angelo Bassi. The schrödinger–newton equation and its foundations. *New Journal of Physics*, 16(11):115007, 2014.
- [45] Richard C Tolman, Paul Ehrenfest, and Boris Podolsky. On the gravitational field produced by light. *Physical Review*, 37(5):602, 1931.
- [46] Dennis Rätzel, Martin Wilkens, and Ralf Menzel. Gravitational properties of light, the gravitational field of a laser pulse. *New Journal of Physics*, 18(2):023009, 2016.
- [47] Richard Howl, Roger Penrose, and Ivette Fuentes. Exploring the unification of quantum theory and general relativity with a bose–einstein condensate. *New Journal of Physics*, 21(4):043047, 2019.
- [48] Sandro Donadi, Luca Ferialdi, and Angelo Bassi. Collapse dynamics are diffusive. *Physical Review Letters*, 130(23):230202, 2023.
- [49] IJ Arnquist, FT Avignone III, AS Barabash, CJ Barton, KH Bhimani, E Blalock, B Bos, M Busch, M Bueck, TS Caldwell, et al. Search for spontaneous radiation from wave function collapse in the majorana demonstrator. *Physical Review Letters*, 129(8):080401, 2022.
- [50] Sandro Donadi, Kristian Piscicchia, Catalina Curceanu, Lajos Diósi, Matthias Laubenstein, and Angelo Bassi. Underground test of gravity-related wave function collapse. *Nature Physics*, 17(1):74–78, 2021.
- [51] Vladislav V Barinov, BT Cleveland, SN Danshin, H Ejiri, SR Elliott, D Frekers, VN Gavrin, VV Gorbachev, DS Gorbunov, WC Haxton, et al. Results from the baksan experiment on sterile transitions (best). *Physical review letters*, 128(23):232501, 2022.
- [52] Steven Ray Elliott, VN Gavrin, and WC Haxton. The gallium anomaly. *Progress in Particle and Nuclear Physics*, page 104082, 2023.
- [53] Raphael Krueger and Thomas Schwetz. Decoherence effects in reactor and gallium neutrino oscillation experiments: a qft approach. *The European Physical Journal C*, 83(7):578, 2023.
- [54] Yasaman Farzan and Thomas Schwetz. A decoherence explanation of the gallium neutrino anomaly. *SciPost Physics*, 15(4):172, 2023.
- [55] Liang-Jian Wen, Jun Cao, and Yi-Fang Wang. Reactor neutrino experiments: present and future. *Annual Review of Nuclear and Particle Science*, 67:183–211, 2017.
- [56] G Mention, M Fechner, Th Lasserre, Th A Mueller, D Lhuillier, M Cribier, and A Letourneau. Reactor antineutrino anomaly. *Physical Review D*, 83(7):073006, 2011.
- [57] Chao Zhang, Xin Qian, and Muriel Fallot. Reactor antineutrino flux and anomaly. *Progress in Particle and Nuclear Physics*, page 104106, 2024.
- [58] Daya Bay, X Guo, et al. A precision measurement of the neutrino mixing angle θ_{13} using reactor antineutrinos at daya-bay. *arXiv preprint hep-ex/0701029*, 2007.
- [59] FP An, JZ Bai, AB Balantekin, HR Band, D Beavis, W Beriguete, M Bishai, S Blyth, K Boddy, RL Brown, et al. Observation of electron-antineutrino disappearance at daya bay. *Physical Review Letters*, 108(17):171803, 2012.
- [60] JH Choi, HI Jang, JS Jang, SH Jeon, KK Joo, K Ju, DE Jung, JG Kim, JH Kim, JY Kim, et al. Search for sub-ev sterile neutrinos at reno. *Physical Review Letters*, 125(19):191801, 2020.
- [61] Y Abe, Christoph Aberle, JC Dos Anjos, JC Barriere, M Bergevin, A Bernstein, TJC Bezerra, L Bezrukhov, E Blucher, NS Bowden, et al. Reactor νe disappearance in the double chooz experiment. *Physical Review D*, 86(5):052008, 2012.
- [62] AA Aguilar-Arevalo, BC Brown, L Bugel, G Cheng, JM Conrad, RL Cooper, R Dharmapalan, A Diaz, Z Djuric, DA Finley, et al. Significant excess of electron-like events in the miniboone short-baseline neutrino experiment. *Physical review letters*, 121(22):221801, 2018.
- [63] P Abratenko, R An, J Anthony, L Arellano, J Asaadi, A Ashkenazi, S Balasubramanian, B Baller, C Barnes, G Barr, et al. Search for an anomalous excess of charged-current νe interactions without pions in the final state with the microboone experiment. *Physical Review D*, 105(11):112004, 2022.
- [64] Serhan Tufanli. The sbnd experiment. In *Proceedings of the XIII International Conference on Heavy Quarks and Leptons (HQL 2016)-New Experiments/Facilities, Blacksburg. PoS*, volume 274, page 70, 2017.
- [65] F Tortorici, V Bellini, C Petta, CM Sutura, Icarus Collaboration, et al. The icarus experiment. *Nuclear and Particle Physics Proceedings*, 306:154–162, 2019.
- [66] R Acciarri, C Adams, R An, C Andreopoulos, AM Ankowski, M Antonello, J Asaadi, W Badgett, L Bagby, B Baibussinov, et al. A proposal for a three detector short-baseline neutrino oscillation program in the fermilab booster neutrino beam. *arXiv preprint arXiv:1503.01520*, 2015.
- [67] AA Aguilar-Arevalo, CE Anderson, AO Bazarko, Stephen J Brice, BC Brown, L Bugel, J Cao, L Coney, JM Conrad, DC Cox, et al. Neutrino flux prediction at miniboone. *Physical Review D*, 79(7):072002, 2009.
- [68] S Avvakumov, T Adams, A Alton, L De Barbaro, P De Barbaro, RH Bernstein, A Bodek, T Bolton, J Brau, D Buchholz, et al. Search for $\nu \mu \rightarrow \nu e$ and $\nu^- \mu \rightarrow \nu^- e$ oscillations at nutev. *Physical Review Letters*, 89(1):011804, 2002.
- [69] JJ Evans et al. The minos experiment: results and prospects. *Advances in High Energy Physics*, 2013, 2013.
- [70] R Acquafredda, T Adam, N Agafonova, P Alvarez Sanchez, M Ambrosio, A Anokhina, S Aoki, A Ariga,

- T Ariga, L Arrabito, et al. The opera experiment in the cern to gran sasso neutrino beam. *Journal of Instrumentation*, 4(04):P04018, 2009.
- [71] MA Acero, P Adamson, L Aliaga, T Alion, V Allakhverdian, N Anfimov, A Antoshkin, Enrique Arrieta-Diaz, A Aurisano, A Back, et al. New constraints on oscillation parameters from ν_e appearance and ν_μ disappearance in the nova experiment. *Physical Review D*, 98(3):032012, 2018.
- [72] K Abe, N Abgrall, H Aihara, Y Ajima, JB Albert, D Allan, P-A Amaudruz, C Andreopoulos, B Andrieu, MD Anerella, et al. The t2k experiment. *Nuclear Instruments and Methods in Physics Research Section A: Accelerators, Spectrometers, Detectors and Associated Equipment*, 659(1):106–135, 2011.
- [73] B Abi, R Acciarri, MA Acero, G Adamov, D Adams, M Adinolfi, Z Ahmad, J Ahmed, T Alion, S Alonso Monsalve, et al. Long-baseline neutrino oscillation physics potential of the dune experiment. *The European Physical Journal C*, 80(10):1–34, 2020.